crystals

MDPI

Article

Raman Scattering as a Probe of the Magnetic State of BEDT-TTF Based Mott Insulators

Nora Hassan [1], Streit Cunningham [1], Elena I. Zhilyaeva [2], Svetlana A. Torunova [2], Rimma N. Lyubovskaya [2], John A. Schlueter [3,4] and Natalia Drichko [1,*]

1 The Institute for Quantum Matter and the Department of Physics and Astronomy, The Johns Hopkins University, Baltimore, MD 21218, USA; nhassan4@jhu.edu (N.H.); streitcunningham@gmail.com (S.C.)
2 Institute of Problems of Chemical Physics, 142432 Chernogolovka, Russia; zhilya@icp.ac.ru (E.I.Z.); torunova@icp.ac.ru (S.A.T.); lyurn@icp.ac.ru (R.N.L.)
3 Division of Materials Research, National Science Foundation, Arlington, VA 22230, USA; jaSchlueter@anl.gov
4 Materials Science Division, Argonne National Laboratory, Argonne, IL 60439, USA
* Correspondence: drichko@jhu.edu; Tel.: +1-410-516-7287

Received: 14 March 2018; Accepted: 16 May 2018; Published: 23 May 2018

Abstract: Quasi-two-dimensional Mott insulators based on BEDT-TTF molecules have recently demonstrated a variety of exotic states, which originate from electron–electron correlations and geometrical frustration of the lattice. Among those states are a triangular $S = 1/2$ spin liquid and quantum dipole liquid. In this article, we show the power of Raman scattering technique to characterize magnetic and electronic excitations of these states. Our results demonstrate a distinction between a spectrum of magnetic excitations in a simple Mott insulator with antiferromagnetic interactions, and a spectrum of an insulator with an additional on-site charge degree of freedom.

Keywords: spin liquid; Raman scattering; BEDT-TTF

1. Introduction

In recent years, a number of materials with very interesting properties produced by electronic correlations have been found among organic conductors and insulators. For example, they present a model to study a bandwidth-controlled transition from Mott insulator to a metal and superconductor, which can be tuned by hydrostatic or chemical pressure in these materials [1,2]. An importance of these studies outside of the community working directly on organic conductors is demonstrated, for example, by the fact that this bandwidth-controlled phase diagram shows a lot of similarity to a doping-dependent phase diagram of electron-doped cuprate superconductors [3].

Recently, much attention was focused on magnetic properties of organic-based Mott insulators on frustrated square and triangular lattices [4]. The number of spin liquid candidates [5–12] with $S = 1/2$ on a triangular lattice found among these materials is larger than among inorganic compounds. Moreover, intriguing ferroelectric properties of spin liquid candidates [13–16], and recently a quantum dipole liquid state [17] were observed for the κ-phase BEDT-TTF-based compounds, where BEDT-TTF stands for bis(ethylenedithio)tetrathiafulvalene. These results suggest an importance of a charge degree of freedom in the Mott insulator state. Theoretical models [18,19] go beyond the simple Mott insulator model that was previously used to describe these materials, and discuss coupling of the charge degree of freedom to spins. In some of the theoretical work, this charge degree of freedom and related effects were discussed within the Kugel–Khomskii model, suggesting a similarity to an orbital liquid [20]. Some of the results still present a conflicting picture; for example, while ferroelectricity

was detected for κ-(BEDT-TTF)$_2$Cu$_2$(CN)$_3$, no evidence of charge disproportionation which would lead to electric dipoles was found [21].

Despite their complicated crystal structure, the electronic structure of these compounds is relatively simple. The layers of the positively charged BEDT-TTF molecules are sandwiched between layers of anions. The anion layers serve as charge reservoirs, but their geometry also influences the structure of the conducting BEDT-TTF layers to some extent. Most of the models which discuss properties of these systems work in an approximation in which electronic and magnetic properties of a material are basically defined by the properties of the BEDT-TTF-based cation layers, the interactions between these layers are very weak if present. These layers can be approximated by a two-dimensional arrangement of "sites". For κ-phase materials discussed in this paper, the cation layer can be mapped on a lattice of molecular dimer sites (BEDT-TTF)$_2^{+1}$ carrying charge $1e$ and spin $1/2$. With high values of electronic correlations U/t, where U is on-cite repulsion and t is transfer integral, these compounds are Mott insulators, and their properties are described by the Hubbard model on 2D square or triangular lattice at half-filling [4,22]. The latter model ignores a possibility of an active intra-dimer degree of freedom, which recently has been found important in some cases [17,18,20]. In a limiting case, the presence of the intra-dimer charge degree of freedom breaks the half-filled model, and a system has to be regarded as $1/4$-filled [19].

In general, much information about a state of matter comes from a knowledge of its excitation spectrum. For example, a lot of our understanding of charge degrees of freedom in organic conductors and insulators is based on the studies of their spectrum of charge excitations. This information was obtained by optical spectroscopy and compared to the calculations on the Hubbard model [2,23]. Measurements of a spectrum of magnetic excitations for organic materials showing interesting magnetic properties present more challenges. A characterization of a spin state by neutron scattering, which by now became a standard tool to study magnetic systems, still has not been performed for these materials due to complicity of the measurements. Until recently, conclusions on the spin liquid behavior in organic Mott insulators on triangular lattice [12] were based on measurements of magnetization, which would suggest J of about 250 K for spin liquid candidates but no magnetic order [24], thermoelectric transport [25] which reveals the presence of mobile excitations assigned to spinons, heat capacity [12], and NMR [26]. However, it is important to directly probe magnetic excitations and obtain the value of J. Also, it is necessary to show that a description of these complicated molecular-based compounds by a simple model of 2D triangular lattice of sites with $S = 1/2$ is valid. Inelastic light scattering technique, so-called Raman scattering, is able to provide this information. This technique is widely used to study magnetic excitations in inorganic systems [27,28]. For example, Raman scattering experiments were a source of information about values of exchange interactions J in cuprate superconductors [29]. Additionally, polarization dependence of magnetic Raman response is a probe of dimensionality and symmetry of a spin system [28,30].

While few different processes can be excited by light in a magnetic system, here we will focus on so-called "exchange Raman scattering" [31], expected in all Heisenberg antiferromegnets (AF). A schematic illustration of this process is presented in Figure 1 for an antiferromagnetically ordered chain. An excitation light of a laser with a frequency ω_L induces an exchange of electrons with opposite spins between the neighboring sites i and j of the two different magnetic sublattices. As a result, a pair of magnons with energies $E_M = \hbar\omega_M$ and wavevectors q and q' so that $q + q' = 0$ is excited. The total energy costs of this process is $E_{2M} = \hbar\omega_{2M}$, thus inelastically scattered light with frequency $\omega_L - \omega_{2M}$ is emitted and collected by a spectrometer. The presented picture describes local excitations and explains sensitivity of the method to short range magnetic correlations. All pairs of magnons with $q + q' = 0$ can be excited, as a result for a system with a long range order the two-magnon Raman spectrum presents a weighted integration of magnon excitations over a Brillouin zone and reflects the renormalized magnon density of states. The position of a two-magnon peak is a direct measure of a magnetic exchange J [29,31]. In the absence of geometrical frustration the peak appears approximately at energy E_{2M}= $J2S(z-1)$, where S is a spin value, and z is a number of nearest neighbors. E_{2M} can

be re-normalized by magnon-magnon interactions. Importantly, a polarization of light in which the excitations are observed is not defined by an easy axis, but by a vector $\delta_{i,j}$ connecting sites i and j of the two different sublattices between which the exchange excitation occurs. Nevertheless, polarization dependence of a two-magnon band in an ordered state reveals the symmetry and dimensionality of the order [28,29].

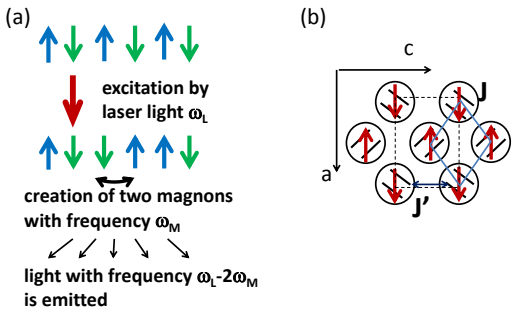

Figure 1. (**a**) A scheme of excitation of pairs of magnons in an antiferromagnetic chain; (**b**) A schematic view of a structure of BEDT-TTF-layer of a κ-phase crystal as a model of $S = 1/2$ sites on a frustrated square lattice.

Theoretical calculations of a magnetic Raman response relevant to organic conductors describe two-magnon excitations on a square and triangular lattice [32,33]. These calculations suggest that as a result of a geometrical frustration, the two-magnon Raman response on a triangular lattice is shifted to lower frequencies compared to the square lattice and looses the distinct polarization dependence of a square lattice, where it is observed only in B_{1g} scattering channel. Both mentioned calculations for a triangular lattice are relevant to a situation where a ground state of an isotropic triangular lattice system is a classical 120° order. Spin excitations spectra were calculated for a model of a triangular lattice with a ring exchange, which actually can produce a spin liquid behavior [34]. While specifically Raman response was not yet calculated, it is clear that in this case, Raman scattering would show a continuum below approximately $4J$.

Publications presenting magnetic Raman scattering in organic conductors started to appear only recently. In this paper, we would like to give an overview of our results on the Raman spectra of magnetic excitations which we observed in a number of κ-phase organic conductors. They demonstrate a striking difference between materials which can be described by a model of a Mott insulator on a frustrated square or triangular lattices with $S = 1/2$ per lattice site, and a more complicated situation, when the intra-dimer charge degree of freedom becomes active, resulting in a quantum dipole liquid [17]. In Section 4 we will compare our results to the existing literature data on other organic spin liquid candidates.

2. Materials and Methods

Raman scattering spectra of single crystals of κ-(BEDT-TTF)$_2$Cu[N(CN)$_2$]Cl, κ-(BEDT-TTF)$_2$Cu[N(CN)$_2$]Br, and κ-(BEDT-TTF)$_2$Hg(SCN)$_2$Br were measured from the plane parallel to BEDT-TTF layers in pseudo-Brewster angle geometry. Measurements were done using T64000 triple monochromator spectrometer equipped with the liquid N_2 cooled CCD detector. For the measurements in the 10–400 cm^{-1} range T64000 in triple monochromator configuration was used. The low frequency cut off was determined by the excitation used and a size of a measured crystal. Crystals of κ-(BEDT-TTF)$_2$Hg(SCN)$_2$Br were not larger than 1 mm by 1mm in the (b, c) plane, the lowest measured frequency for these crystals was 20 cm^{-1}. For the measurements in the range 100–2000 cm^{-1} single monochromator configuration with the edge filter option was used. Spectral resolution was 2 cm^{-1}. Lines of Ar^+-Kr^+ Coherent laser at 514.5 nm and 647 nm where used for excitation. Laser power was kept at 2 mW for the laser probe size of approximately 50 by 100 μm. This ensured that the laser heating of the sample was kept below 2 K. Measurements at temperatures down to 10 K were

performed using Janis ST500 cold finger cryostat. Cooling rates used were between 0.2 and 0.5 K/min. The samples were glued on the cold finger of the cryostat using GE varnish. The experiments were performed on at least 6 samples to ensure reproducibility of the results. The crystals were oriented using polarization-dependent Raman scattering measurements.

For the measurements, electrical vector of excitation e_L and scattered e_S light were polarized along the in-plane crystallographic axes (a and c for κ-(BEDT-TTF)$_2$Cu[N(CN)$_2$]Cl and κ-(BEDT-TTF)$_2$Cu[N(CN)$_2$]Br, and b and c axes for κ-(BEDT-TTF)$_2$Hg(SCN)$_2$Br). Our notations of polarizations refer to the structure and symmetry of the BEDT-TTF layer, to make an easy comparison to the calculations which refer to D_{4h} [29] without loosing the information about the symmetry of the real crystal. Thus A_{1g} symmetry corresponds to measurements in (b,b) and (c,c) geometries, and B_{1g} corresponds to (b,c) and (c,b) geometries (xy). All spectra were corrected by the Bose-Einstein thermal factor.

Raman spectra of organic conductors are a complicated spectra with an overlap of molecular vibrations, lattice phonons, some effect of electron-molecular vibrational coupling, electronic and magnetic excitations, and luminescence. At this point vibrational contributions [35,36] and luminescence [37] are well understood and can be subtracted from the spectra. In order to do so we fitted the phonons with the Lorentz functions, and luminescence with broad Lorentz bands located at 5000 cm^{-1} for all materials, and additionally a weaker band located at 3000 cm^{-1} for Mott insulators, basing on the results of Ref. [38]. For the materials of κ-Cu family, the identical luminescence contribution, normalized on the phonons intensity, was subtracted from all the spectra.

3. Results

An overview of the Raman spectra of the four discussed κ-phase compounds κ-(BEDT-TTF)$_2$Cu[N(CN)$_2$]Cl, κ-(BEDT-TTF)$_2$Cu[N(CN)$_2$]Br, κ-(BEDT-TTF)$_2$Cu$_2$(CN)$_3$, and κ-(BEDT-TTF)$_2$Hg(SCN)$_2$Br is presented in Figure 2. We show the data obtained at low temperatures around 10 K for two polarizations which would correspond to A_{1g} and B_{1g} scattering channels in a square magnetic unit cell of κ-(BEDT-TTF)$_2$Cu[N(CN)$_2$]Cl (Figure 1b). The range from 100 to 1600 cm^{-1} covers the frequency range where we can observe two-magnon continuum for a square lattice with J of around a few hundred kelvin.

The insets in Figure 2 show original data, and reveal a complicated picture. Multiple narrow bands observed in the spectra belong to molecular vibrations of BEDT-TTF and lattice vibrations [35,36]. They are superimposed on a background which consist of luminescence [38], possible electronic excitations, and magnetic excitations. A spectrum of phonons which do not interact with electronic and magnetic degrees of freedom is easy to interpret and subtract from the original data. While a maximum of luminescence is observed at much higher frequencies of 3000 cm^{-1} for all the compounds, it does appear in the spectra as a nearly linear background with different intensity for these four materials. Luminescence shows the larger intensity in polarizations, where electrical vector e_L of the excitation light is parallel to the crystallograpic direction which has a projection of the long axis of BEDT-TTF molecule, thus we always selected polarizations with the smaller luminescence intensity. An additional luminescence signal comes from a maximum at around 5000 cm^{-1} [38], and apparently belongs to the response of an anion layer. It is much stronger in κ-(BEDT-TTF)$_2$Hg(SCN)$_2$Br spectra.

In cross-polarization (B_{1g} scattering channel) we could successfully disentangle luminescence and the electronic or magnetic background, but in A_{1g} scattering channel of κ-Cu-family materials some higher-frequency component is left. This can be an electronic response of a system, for example transitions between Hubbard bands. For D_{4h} symmetry which we use to approximate the structure of κ-phase BEDT-TTF layer, electronic contribution would be present in both A_{1g} and B_{1g} channels, while absent in B_{2g} [29,38]. Since electronic response in A_{1g} scattering channel is proportional to the intensity of electronic transitions integrated over the whole BZ [29], the electronic contunuum is typically more intense in A_{1g} channel [39].

In most cases, a distinct polarization dependence and frequency range of magnetic excitations allow to separate them from other contributions. In the relevant section, we will discuss a particular difficulty of the analysis of the data in A_{1g} scattering channel for κ-(BEDT-TTF)$_2$Cu$_2$(CN)$_3$.

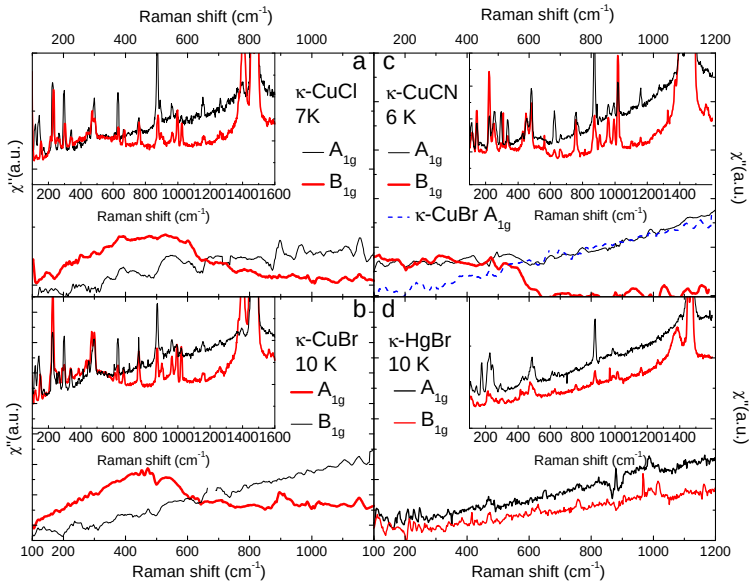

Figure 2. Low temperature Raman spectra for the discussed κ phase materials in the spectral range between 100 and 1600 cm^{-1} in polarizations corresponding to A_{1g} and B_{1g} in D_{4h} symmetry. The insets show original data, the main figures show data with phonons and luminescence contribution subtracted. The resulting spectra, containing magnetic and, possibly, electronic contributions are plotted (**a**) Spectra of κ-(BEDT-TTF)$_2$Cu[N(CN)$_2$]Cl at 7 K. Note the broad maximum in B_{1g} symmetry between 100 and 700 cm^{-1}; (**b**) Spectra of κ-(BEDT-TTF)$_2$Cu[N(CN)$_2$]Br at 10 K. Note the broad maximum in B_{1g} symmetry between 100 and 700 cm^{-1}, similar to κ-(BEDT-TTF)$_2$Cu[N(CN)$_2$]Cl; (**c**) Spectra of κ-(BEDT-TTF)$_2$Cu$_2$(CN)$_3$ at 6 K. The continuum extends from about 600 cm^{-1} to the lowest measured frequencies, no gap in magnetic spectrum can be identified, in contrast to κ-(BEDT-TTF)$_2$Cu[N(CN)$_2$]Cl and κ-(BEDT-TTF)$_2$Cu[N(CN)$_2$]Br. The dashed line shows A_{1g} contribution of κ-(BEDT-TTF)$_2$Cu[N(CN)$_2$]Br for comparison, which makes clear the presence of an additional intensity below 600 cm^{-1} in A_{1g} for κ-(BEDT-TTF)$_2$Cu$_2$(CN)$_3$, which we attribute to magnetic excitations; (**d**) Spectra of κ-(BEDT-TTF)$_2$Hg(SCN)$_2$Br at 10 K, the spectra do not show major differences between A_{1g} and B_{1g} channels in the discussed range, no continuum of magnetic excitations is observed.

3.1. Magnetic Excitations on a Frustrated Square Lattice: From a Mott Insulator with an Antiferromagnetic Order to a Metal with Antiferromagnetic Fluctuations

A simple and well-understood example of magnetic excitations in an organic Mott insulator are spectra of an AF state for κ-(BEDT-TTF)$_2$Cu[N(CN)$_2$]Cl (T_N = 27 K). In the Raman response of this compound (see Figure 2a) we observe a broad maximum between 200 and 700 cm^{-1} only in (a,c) polarization, which corresponds to B_{1g} symmetry of the magnetic unit cell in κ-(BEDT-TTF)$_2$Cu[N(CN)$_2$]Cl (see Figure 1b). This maximum is absent in (c,c) spectra, which correspond to A_{1g} symmetry (Figure 2a), as well as in B_{2g} [38]. This polarization dependence coincides with the theoretical expectations for a two-magnon response of AF order on a square lattice. Any electronic excitations due to correlation effects would be observed both in A_{1g} and B_{1g} channels [29] and are expected at higher frequencies [2]. The contribution observed in (c,c) polarization is a good candidate for the electronic contribution to the spectra. In Ref. [32] two-magnon Raman response of an AF on a frustrated square lattice described by a Hubbard model was calculated depending on the frustration parameter J'/J. For $J'/J = 0.22$ [38] a two-magnon excitation would be

observed in B_{1g} polarization only, with a maximum at about $2.5J$. This provides us an estimate of $J = 250$ K, close to that obtained from the fit of magnetization [24].

The κ-(BEDT-TTF)$_2$Cu[N(CN)$_2$]Br metal with superconducting transition below $T = 11.5$ K demonstrates electronic parameters very similar to that of κ-(BEDT-TTF)$_2$Cu[N(CN)$_2$]Cl. Only a small decrease in U/t value is responsible for tuning this material into metallic and superconducting states [4]. While electronic spectra of these compounds are very different, reflecting the difference in the charge ground states [2], κ-(BEDT-TTF)$_2$Cu[N(CN)$_2$]Cl and κ-(BEDT-TTF)$_2$Cu[N(CN)$_2$]Br show an amazing similarity in the spectrum of magnetic excitations (see Figure 2b), which has a similar position, shape, and polarization dependence. It is therefore natural to assign the maximum present in the spectra of κ-(BEDT-TTF)$_2$Cu[N(CN)$_2$]Br between 200 and 700 cm^{-1} only in B_{1g} scattering channel, to magnetic excitations due to local AF correlations. The presence of AF fluctuations below 200 K in κ-(BEDT-TTF)$_2$Cu[N(CN)$_2$]Br was observed also by other methods [40].

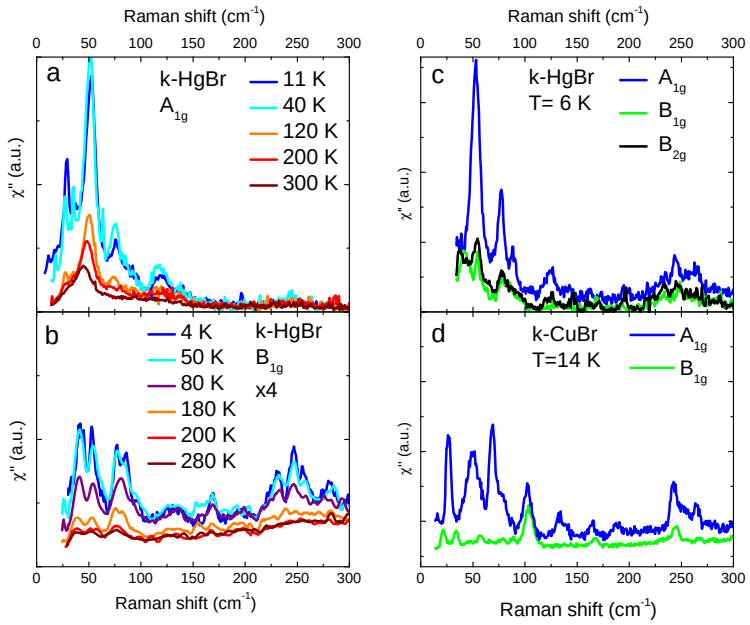

Figure 3. (**a**,**b**) Temperature dependence of Raman spectra of κ-(BEDT-TTF)$_2$Hg(SCN)$_2$Br in the range below 300 cm^{-1} in (**a**) A_{1g} scattering channel; and (**b**) B_{1g} scattering channel, intensity is multiplied by the factor of 4; (**c**) Polarization dependence of the low-frequency spectra for κ-(BEDT-TTF)$_2$Hg(SCN)$_2$Br at 4 K; (**d**) Polarization dependence of low frequency spectra of κ-(BEDT-TTF)$_2$Cu[N(CN)$_2$]Br at 14 K. Note the absence of the broad mode with the maximum at about 40 cm^{-1}.

To summarize, as a whole, Raman spectra of magnetic excitations in κ-(BEDT-TTF)$_2$Cu[N(CN)$_2$]Cl and κ-(BEDT-TTF)$_2$Cu[N(CN)$_2$]Br are in agreement with the calculations for an AF on a frustrated square lattice with $S = 1/2$, and reproduce the value of J received from magnetization measurements. Some details of temperature and U/t dependence of the spectra are unconventional. (i) An extreme similarity between magnetic excitations of an AF ordered κ-(BEDT-TTF)$_2$Cu[N(CN)$_2$]Cl and metallic κ-(BEDT-TTF)$_2$Cu[N(CN)$_2$]Br with AF fluctuations is unexpected. Typically, in a metallic state next to a Mott insulator, where AF fluctuations survive, a two-magnon peak is broadened and shifted down in frequencies due to the interactions with charge carriers [29]; (ii) As we have shown in Ref. [38], the two-magnon peak fully forms in κ-(BEDT-TTF)$_2$Cu[N(CN)$_2$]Cl at around 50 K, and does not change when the material is cooled through the ordering transition at $T_N = 27$ K. This is in contrast to the majority of magnetic materials, where the two-magnon peak would shift to higher frequencies and become more narrow below T_N [27]. While the details of this behavior still need an explanation, it is clear that two-dimensional magnetic interactions, and high energy scale of J compared to the

temperature of ordering and to the energy scale where charge carriers are observed, lie at the origin of these effects.

3.2. Mott Insulator on a Triangular Lattice: κ-(BEDT-TTF)$_2$Cu$_2$(CN)$_3$

The overall spectra of κ-(BEDT-TTF)$_2$Cu$_2$(CN)$_3$ are similar to that of the two materials discussed above, but show a difference in the position of the band assigned to the two-magnon excitations. In the spectra of κ-(BEDT-TTF)$_2$Cu$_2$(CN)$_3$ in (a,c). polarization (Figure 2c) we observe a broad feature below approximately 600 cm^{-1} which we assign to magnetic excitations. Interestingly, the band of magnetic excitations is extended to much lower frequencies than in the less frustrated materials κ-(BEDT-TTF)$_2$Cu[N(CN)$_2$]Cl and κ-(BEDT-TTF)$_2$Cu[N(CN)$_2$]Br, and is still present at the lowest measured frequency of 50 cm^{-1}. The low frequency shift of the two-magnon peak is in a good agreement with a calculation of the two-magnon peak position for a model of $S = 1/2$ on frustrated square lattice with frustration value of J'/J = 0.64 [32,41]. Assuming the value of J value of κ-(BEDT-TTF)$_2$Cu$_2$(CN)$_3$ close to that of κ-(BEDT-TTF)$_2$Cu[N(CN)$_2$]Cl, the center of two-magnon peak should shift to about 230 cm^{-1}. However, this calculation discusses a classical picture of 120° order as a ground state of an AF on an isotropic triangular lattice, which is not the case for κ-(BEDT-TTF)$_2$Cu$_2$(CN)$_3$. Another recently discussed explanation of a spin liquid state in κ-(BEDT-TTF)$_2$Cu$_2$(CN)$_3$ is a model of a triangular lattice with a ring exchange [34]. Ring exchange is suggested as the largest exchange of the next order beyond a nearest neighbor exchange J and destroys the ordered ground state. A spectrum of magnetic excitations of this spin liquid state is discussed in Ref. [34], and would produce a continuum of excitations below about $4J$. We observe a continuum of excitations in κ-(BEDT-TTF)$_2$Cu$_2$(CN)$_3$ spectra below 600 cm^{-1}, which gives an estimate of J of about 215 K, in a good agreement with other measurements. While producing different low temperature states, these two models agree on a starting model of a $S = 1/2$ AF on triangular lattice, with no active charge degree of freedom.

Calculations [32,33] predict a loss of anisotropy between the two-magnon continuum in B_{1g} and A_{1g} scattering channels for an isotropic triangular lattice. We find that this loss of polarization dependence makes it more challenging to separate magnetic excitations from possible electronic and luminescence background in A_{1g} scattering channel. A work of Nakamura et al. [41] suggest small intensity of magnetic Raman scattering in this channel. Indeed, using a fit of luminescence background, parameters for which is very difficult to restrict, one receives a very low intensity of magnetic scattering in A_{1g}. On the other hand, a comparison of (c,c) spectra with that of κ-(BEDT-TTF)$_2$Cu[N(CN)$_2$]Br and κ-(BEDT-TTF)$_2$Cu[N(CN)$_2$]Cl suggest an additional intensity in κ-(BEDT-TTF)$_2$Cu$_2$(CN)$_3$ spectra at low frequencies (see Figure 2), which we assign to magnetic excitations. At this point, the error bars for the intensity of magnetic excitations in A_{1g} scattering channel are large, but the presence of these excitations is in agreement with the symmetry of the lattice.

3.3. Charge Degree of Freedom in a Mott Insulator: κ-(BEDT-TTF)$_2$Hg(SCN)$_2$Br

κ-(BEDT-TTF)$_2$Hg(SCN)$_2$Br shows κ-phase structure, where the layer formed by the (BEDT-TTF)$_2^{+1}$ dimers is well approximated by an anisotropic triangular lattice with the ratio of t'/t at least as high as for κ-(BEDT-TTF)$_2$Cu$_2$(CN)$_3$. In a Mott insulator, where J is estimated as $J = 4t^2/U$, this would result in a similarly high magnetic frustration. Calculations carried out for an iso-structural κ-(BEDT-TTF)$_2$Hg(SCN)$_2$Cl compound suggest values of t and t' similar to Cu-based κ-phases, but a slightly lower degree of dimerisation [37,42]. Contrary to the expectation based on a model of a Mott insulator with $S = 1/2$ on a triangular lattice, no continuum of magnetic excitations in the range between 100 and 700 cm^{-1} is observed in the spectra (see Figure 2d).

The reason for this difference is an "active" intra-dimer degree of freedom. Indeed, in contrast to the compounds discussed in the previous section, κ-(BEDT-TTF)$_2$Hg(SCN)$_2$Br shows an evidence of fluctuating intra-dimer charge detected by vibrational spectroscopy [17]. Respectively, a different collective excitation with a maximum at around 40 cm^{-1} is found in the spectra of this compound.

It appears in both polarizations at temperatures below the Mott transition [43] at 80 K (Figure 3a,b). This excitation is attributed [17] to a collective excitation of dipoles fluctuating on $(BEDT\text{-}TTF)_2^{+1}$ dimers in the insulating state of κ-$(BEDT\text{-}TTF)_2Hg(SCN)_2Br$, forming "quantum dipole liquid".

Additional understanding of the low frequency region of the spectra comes from a comparison of spectra of κ-$(BEDT\text{-}TTF)_2Cu[N(CN)_2]Br$ at 14 K with the spectra of κ-$(BEDT\text{-}TTF)_2Hg(SCN)_2Br$ in this range (Figure 3c,d) at the lowest measured temperature of 4 K. For κ-$(BEDT\text{-}TTF)_2Cu[N(CN)_2]Br$ this frequency range is below the range where magnetic excitations are observed, but above spectral range where the superconducting gap can appear [29], thus we do not expect any electronic or magnetic excitations. In the Raman spectra at low frequencies of BEDT-TTF-based compounds we typically observe bands of vibrations of the BEDT-TTF molecule down to approximately 100 cm^{-1} [35]. They are found at similar frequencies for various BEDT-TTF-based crystals, for example bands at around 250 cm^{-1} and a phonon at 125 cm^{-1}, observed for both κ-$(BEDT\text{-}TTF)_2Hg(SCN)_2Br$ and κ-$(BEDT\text{-}TTF)_2Cu[N(CN)_2]Br$ (Figure 3c,d). The phonons in the range below approximately 100 cm^{-1} are lattice vibrations [36]. Their frequency depends on the details of the structure of the crystals, including that of the anion. For κ-phase BEDT-TTF-based crystals similar modes exist, for example modes at about 50 and 75 cm^{-1} are present in the A_{1g} scattering channel for both compounds.

For κ-$(BEDT\text{-}TTF)_2Hg(SCN)_2Br$ in A_{1g} , the intense low frequency phonons are superimposed on a broad background mode of dipole fluctuations [17]. The collective excitation is not coupled to the A_{1g} phonons. This fact allows us to subtract the phonons from the original spectra in order to extract the information about the mode itself [17]. In B_{1g} polarization, the spectrum of κ-$(BEDT\text{-}TTF)_2Cu[N(CN)_2]Br$ is overall flat with weak phonon bands below 40 cm^{-1}. In contrast, the spectra of κ-$(BEDT\text{-}TTF)_2Hg(SCN)_2Br$ show the background mode, and asymmetric bands of phonons at about 40 and 80 cm^{-1}. These asymmetric Fano shape of the phonons evidences for the coupling of these phonons with the underlying continuum, which makes it challenging to separate the phonons and the collective mode contributions.

At this point, there are no calculations which address the origin of the excitation observed in the low-frequency spectra of κ-$(BEDT\text{-}TTF)_2Hg(SCN)_2Br$, and its assignment to the collective excitation of dipoles localised on $(BEDT\text{-}TTF)_2^{+1}$ dimers is based on experimental data. Thus, the symmetry of this excitations, and the involvement of spin excitations are not yet understood. However, an identification of the phonons which are coupled to this excitation are important. Lattice phonons can define the formation of a low-temperature state by modulation of transfer integrals which define magnetic exchange J, as well as the U/t and V/t correlation values which are important for electric dipole formation.

4. Discussion

We present our results on the Raman spectra of four κ-phase BEDT-TTF-based compounds. While Raman spectra of these materials are very rich, our discussion focuses on magnetic Raman excitations. These κ-phase materials have very similar structures of BEDT-TTF layers, with well-defined dimers of $(BEDT\text{-}TTF)_2^{+1}$ molecules forming frustrated square or anisotropic triangular lattices. Our data reveal a presence of magnetic Raman excitations in the frequency range of 50–700 cm^{-1} in the spectra of AF ordered κ-$(BEDT\text{-}TTF)_2Cu[N(CN)_2]Cl$, metal with AF fluctuations κ-$(BEDT\text{-}TTF)_2Cu[N(CN)_2]Br$, and spin liquid candidate κ-$(BEDT\text{-}TTF)_2Cu_2(CN)_3$. These excitations can be understood within a model of an AF Mott insulator with $S = 1/2$. For κ-$(BEDT\text{-}TTF)_2Cu[N(CN)_2]Cl$ and κ-$(BEDT\text{-}TTF)_2Cu[N(CN)_2]Br$ polarization dependence supports an approximation of the magnetic structure by a weakly frustrated square lattice. Position of the continuum of magnetic excitations in the spectral region of around 200-700 cm^{-1} is in agreement with the estimate of J of about 250 K. Excitations in κ-$(BEDT\text{-}TTF)_2Cu_2(CN)_3$ spectra are shifted down in frequency, as expected for a triangular lattice, and are observed down to the lowest measured frequencies, suggesting a broader continuum than for the other two materials. In addition to a simple model of $S = 1/2$ on a triangular lattice with AF nearest neighbor interactions, and a triangular lattice

with nearest neighbor and ring exchange, a recent work [44] suggested a dynamic low-dimensionality of the magnetic interactions in κ-(BEDT-TTF)$_2$Cu$_2$(CN)$_3$ as an alternative explanation for the spin liquid behaviour. One of the ways to distinguish which model describes well κ-(BEDT-TTF)$_2$Cu$_2$(CN)$_3$ is to reproduce the Raman spectra of magnetic excitations for this system. Importantly, all these models developed for κ-(BEDT-TTF)$_2$Cu$_2$(CN)$_3$ do not include an on-site charge degree of freedom.

Another recently suggested spin liquid candidate which belongs to the family of organic Mott insulators on a triangular lattice is κ-(BEDT-TTF)$_2$Ag$_2$(CN)$_3$. Magnetic Raman scattering spectra of this material are presented in Ref. [45], and show a lot of similarity to κ-(BEDT-TTF)$_2$Cu$_2$(CN)$_3$, with a continuum of magnetic excitations found below about 600 cm^{-1}. These data suggest that this system also fits into the model of (BEDT-TTF)$_2^{+1}$ dimer sites with $S = 1/2$ on a triangular lattice.

Unexpectedly, κ-(BEDT-TTF)$_2$Hg(SCN)$_2$Br shows a completely different spectrum of excitations. The fact that no continuum of magnetic excitations was found in the spectral range 50–600 cm^{-1} in its Raman spectra immediately suggested that a simple description of a Mott insulator with a triangular lattice of dimer sites with $S = 1/2$ and J of about 250 K fails in this case. Instead, a collective mode at much lower energies below 100 cm^{-1} appears in the low temperature spectra, with polarization dependence suggesting an electronic origin of the mode. We have shown in Ref. [17] that this mode is a collective excitation of dipoles fluctuating on (BEDT-TTF)$_2^{+1}$ dimer sites. An absence of the two-magnon band is also recorded for κ-(BEDT-TTF)$_2$Hg(SCN)$_2$Cl, a compound basically isostructural to κ-(BEDT-TTF)$_2$Hg(SCN)$_2$Br but showing a charge ordered state below $T = 30$ K [17].

A similar picture was observed in the spectra of β' materials based on the Pd(dmit)$_2$ molecule [46]. While an AF ordered Me$_4$P[Pd(dmit)$_2$]$_2$ and a spin liquid candidate EtMe$_3$Sb[Pd(dmit)$_2$]$_2$ show a continuum of magnetic excitations in their Raman spectra, it is absent in the spectra of a charge ordered analog Et$_2$Me$_2$Sb[Pd(dmit)$_2$]$_2$.

To summarize, we demonstrate that magnetic Raman response provides a unique direct measure of a value of the magnetic exchange J for a number of BEDT-TTF-based materials, and the understanding of an origin of magnetic excitations in these compounds. It shows that κ-(BEDT-TTF)$_2$Cu[N(CN)$_2$]Cl, κ-(BEDT-TTF)$_2$Cu[N(CN)$_2$]Br, κ-(BEDT-TTF)$_2$Cu$_2$(CN)$_3$, κ-(BEDT-TTF)$_2$Ag$_2$(CN)$_3$, Me$_4$P[Pd(dmit)$_2$]$_2$, and EtMe$_3$Sb[Pd(dmit)$_2$]$_2$ are well described by a model of $S = 1/2$ spins on a square or triangular lattice. In contrast, κ-(BEDT-TTF)$_2$Hg(SCN)$_2$Br, κ-(BEDT-TTF)$_2$Hg(SCN)$_2$Cl, and Et$_2$Me$_2$Sb[Pd(dmit)$_2$]$_2$ posses an active intra-dimer charge degree of freedom, the presence of which completely changes the magnetic excitation spectra. The fluctuating charge degree of freedom in a quantum spin liquid is suggested to produce a new kind of spin liquid in a presence of charge-spin coupling [18,20].

Author Contributions: N.D. conceived and designed the experiments; N.H., S.C. and N.D. performed the experiments and data analysis; J.A.S., S.A.T., E.I.Z. and R.N.L. contributed characterized samples.

Acknowledgments: The work at Institute of Quantum Matter was supported by the U.S. Department of Energy, Office of Basic Energy Sciences, Division of Material Sciences and Engineering under Grant No. DE-FG02-08ER46544. The work in Chernogolovka was supported by FASO Russia, state task state registration number 0089-2014-0036. J.A.S. acknowledges support from the Independent Research and Development program from the NSF while working at the Foundation and from the National High Magnetic Field Laboratory (NHMFL) User Collaboration Grants Program (UCGP). Work at ANL was supported by University of Chicago Argonne, LLC, Operator of Argonne National Laboratory ("Argonne") Argonne, a U.S. Department of Energy Office of Science laboratory, is operated under Contract No. DE-AC02-06CH11357.

Conflicts of Interest: The authors declare no conflict of interest.

References

1. Lefebvre, S.; Wzietek, P.; Brown, S.; Bourbonnais, C.; Jérome, D.; Mézière, C.; Fourmigué, M.; Batail, P. Mott Transition, Antiferromagnetism, and Unconventional Superconductivity in Layered Organic Superconductors. *Phys. Rev. Lett.* **2000**, *85*, 5420–5423.
2. Faltermeier, D.; Barz, J.; Dumm, M.; Dressel, M.; Drichko, N.; Petrov, B.; Semkin, V.; Vlasova, R.; Meźière, C.; Batail, P. Bandwidth-controlled Mott transition in κ-(BEDT-TTF)$_2$Cu[N(CN)$_2$]Br$_x$Cl$_{1-x}$: Optical studies of localized charge excitations. *Phys. Rev. B* **2007**, *76*, 165113.

3. Armitage, N.P.; Fournier, P.; Greene, R.L. Progress and perspectives on electron-doped cuprates. *Rev. Mod. Phys.* **2010**, *82*, 2421–2487. [CrossRef]
4. Powell, B.J.; McKenzie, R.H. Quantum frustration in organic Mott insulators: from spin liquids to unconventional superconductors. *Rep. Prog. Phys.* **2011**, *74*, 056501.
5. Balents, L. Spin liquids in frustrated magnets. *Nature* **2010**, *464*, 199–208. [CrossRef] [PubMed]
6. Yamashita, S.; Nakazawa, Y.; Oguni, M.; Oshima, Y.; Nojiri, H.; Shimizu, Y.; Miyagawa, K.; Kanoda, K. Thermodynamic properties of a spin-1/2 spin-liquid state in a κ-type organic salt. *Nat. Phys.* **2008**, *4*, 459–462.
7. Yamashita, S.; Yamamoto, T.; Nakazawa, Y.; Tamura, M.; Kato, R. Gapless spin liquid of an organic triangular compound evidenced by thermodynamic measurements. *Nat. Commun.* **2011**, *2*, 275. [CrossRef] [PubMed]
8. Yamashita, S.; Nakazawa, Y. Heat capacities of antiferromagnetic dimer-Mott insulators in organic charge-transfer complexes. *J. Therm. Anal. Calorim.* **2010**, *99*, 153–157. [CrossRef]
9. Pratt, F.; Baker, P.; Blundell, S.; Lancaster, T.; Ohira-Kawamura, S.; Baines, C.; Shimizu, Y.; Kanoda, K.; Watanabe, I.; Saito, G. Magnetic and non-magnetic phases of a quantum spin liquid. *Nature* **2011**, *471*, 612–616. [CrossRef] [PubMed]
10. Isono, T.; Kamo, H.; Ueda, A.; Takahashi, K.; Kimata, M.; Tajima, H.; Tsuchiya, S.; Terashima, T.; Uji, S.; Mori, H. Gapless Quantum Spin Liquid in an Organic Spin-1/2 Triangular-Lattice κ-H_3(Cat-EDT-TTF)$_2$. *Phys. Rev. Lett.* **2014**, *112*, 177201.
11. Shimizu, Y.; Hiramatsu, T.; Maesato, M.; Otsuka, A.; Yamochi, H.; Ono, A.; Itoh, M.; Yoshida, M.; Takigawa, M.; Yoshida, Y.; et al. Pressure-Tuned Exchange Coupling of a Quantum Spin Liquid in the Molecular Triangular Lattice κ-$(ET)_2Ag_2(CN)_3$. *Phys. Rev. Lett.* **2016**, *117*, 107203. [CrossRef] [PubMed]
12. Zhou, Y.; Kanoda, K.; Ng, T.K. Quantum spin liquid states. *Rev. Mod. Phys.* **2017**, *89*, 025003. [CrossRef]
13. Abdel-Jawad, M.; Terasaki, I.; Sasaki, T.; Yoneyama, N.; Kobayashi, N.; Uesu, Y.; Hotta, C. Anomalous dielectric response in the dimer Mott insulator κ-(BEDT-TTF)$_2$Cu$_2$(CN)$_3$. *Phys. Rev. B* **2010**, *82*, 125119. [CrossRef]
14. Lunkenheimer, P.; Müller, J.; Krohns, S.; Schrettle, F.; Loidl, A.; Hartmann, B.; Rommel, R.; De Souza, M.; Hotta, C.; Schlueter, J.A.; et al. Multiferroicity in an organic charge-transfer salt that is suggestive of electric-dipole-driven magnetism. *Nat. Mater.* **2012**, *11*, 755–758. [CrossRef] [PubMed]
15. Tomić, S.; Pinterić, M.; Ivek, T.; Sedlmeier, K.; Beyer, R.; Wu, D.; Schlueter, J.; Schweitzer, D.; Dressel, M. Magnetic ordering and charge dynamics in κ-(BEDT-TTF)$_2$Cu[N(CN)$_2$] Cl. *J. Phys. Condens. Matter* **2013**, *25*, 436004. [CrossRef] [PubMed]
16. Pinterić, M.; Čulo, M.; Milat, O.; Basletić, M.; Korin-Hamzić, B.; Tafra, E.; Hamzić, A.; Ivek, T.; Peterseim, T.; Miyagawa, K.; et al. Anisotropic charge dynamics in the quantum spin-liquid candidate κ-$(BEDT\text{-}TTF)_2Cu_2(CN)_3$. *Phys. Rev. B* **2014**, *90*, 195139. [CrossRef]
17. Hassan, N.; Cunningham, S.; Mourigal, M.; Zhilyaeva, E.I.; Torunova, S.A.; Lyubovskaya, R.N.; Drichko, N. Observation of a quantum dipole liquid state in an organic quasi-two-dimensional material. *Science* **2018**, arXiv:1704.04482.
18. Hotta, C. Quantum electric dipoles in spin-liquid dimer Mott insulator κ-$ET_2Cu2(CN)_3$. *Phys. Rev. B* **2010**, *82*, 241104. [CrossRef]
19. Dayal, S.; Clay, R.T.; Li, H.; Mazumdar, S. Paired electron crystal: Order from frustration in the quarter-filled band. *Phys. Rev. B* **2011**, *83*, 245106.
20. Naka, M.; Ishihara, S. Quantum melting of magnetic order in an organic dimer Mott-insulating system. *Phys. Rev. B* **2016**, *93*, 195114. [CrossRef]
21. Sedlmeier, K.; Elsässer, S.; Neubauer, D.; Beyer, R.; Wu, D.; Ivek, T.; Tomić, S.; Schlueter, J.A.; Dressel, M. Absence of charge order in the dimerized κ-phase BEDT-TTF salts. *Phys. Rev. B* **2012**, *86*, 245103. [CrossRef]
22. Seo, H.; Hotta, C.; Fukuyama, H. Toward Systematic Understanding of Diversity of Electronic Properties in Low-Dimensional Molecular Solids. *Chem. Rev.* **2004**, *104*, 5005–5036. [CrossRef] [PubMed]
23. Merino, J.; Dumm, M.; Drichko, N.; Dressel, M.; McKenzie, R.H. Quasiparticles at the Verge of Localization near the Mott Metal-Insulator Transition in a Two-Dimensional Material. *Phys. Rev. Lett.* **2008**, *100*, 086404. [CrossRef] [PubMed]
24. Shimizu, Y.; Miyagawa, K.; Kanoda, K.; Maesato, M.; Saito, G. Spin liquid state in an organic Mott insulator with a triangular lattice. *Phys. Rev. Lett.* **2003**, *91*, 107001. [CrossRef] [PubMed]

25. Yamashita, M.; Nakata, N.; Senshu, Y.; Nagata, M.; Yamamoto, H.M.; Kato, R.; Shibauchi, T.; Matsuda, Y. Highly mobile gapless excitations in a two-dimensional candidate quantum spin liquid. *Science* **2010**, *328*, 1246–1248. [CrossRef] [PubMed]
26. Shimizu, Y.; Miyagawa, K.; Kanoda, K.; Maesato, M.; Saito, G. Emergence of inhomogeneous moments from spin liquid in the triangular-lattice Mott insulator κ-$(ET)_2Cu_2(CN)_3$. *Phys. Rev. B* **2006**, *73*, 140407. [CrossRef]
27. Cottam, M.G.; Lockwood, D.J. *Light Scattering in Magnetic Solids*; Wiley: New York, NY, USA, 1986.
28. Lemmens, P.; Güntherodt, G.; Gros, C. Magnetic light scattering in low-dimensional quantum spin systems. *Phys. Rep.* **2003**, *375*, 1–103. [CrossRef]
29. Devereaux, T.P.; Hackl, R. Inelastic light scattering from correlated electrons. *Rev. Mod. Phys.* **2007**, *79*, 175.
30. Chen, C.C.; Jia, C.J.; Kemper, A.F.; Singh, R.R.P.; Devereaux, T.P. Theory of Two-Magnon Raman Scattering in Iron Pnictides and Chalcogenides. *Phys. Rev. Lett.* **2011**, *106*, 067002.
31. Fleury, P.; Loudon, R. Scattering of light by one-and two-magnon excitations. *Phys. Rev.* **1968**, *166*, 514.
32. Vernay, F.; Devereaux, T.; Gingras, M. Raman scattering for triangular lattices spin-1/2 Heisenberg antiferromagnets. *J. Phys. Condens. Matter* **2007**, *19*, 145243.
33. Perkins, N.; Brenig, W. Raman scattering in a Heisenberg $S = \frac{1}{2}$ antiferromagnet on the triangular lattice. *Phys. Rev. B* **2008**, *77*, 174412.
34. Holt, M.; Powell, B.J.; Merino, J. Spin-liquid phase due to competing classical orders in the semiclassical theory of the Heisenberg model with ring exchange on an anisotropic triangular lattice. *Phys. Rev. B* **2014**, *89*, 174415. [CrossRef]
35. Kozlov, M.; Pokhodnia, K.; Yurchenko, A. The assignment of fundamental vibrations of BEDT-TTF and BEDT-TTF-d8. *Spectrochim. Acta Part A Mol. Spectrosc.* **1987**, *43*, 323–329. [CrossRef]
36. Dressel, M.; Lazić, P.; Pustogow, A.; Zhukova, E.; Gorshunov, B.; Schlueter, J.A.; Milat, O.; Gumhalter, B.; Tomić, S. Lattice vibrations of the charge-transfer salt κ-$(BEDT\text{-}TTF)_2Cu_2(CN)_3$: Comprehensive explanation of the electrodynamic response in a spin-liquid compound. *Phys. Rev. B* **2016**, *93*, 081201. [CrossRef]
37. Drichko, N.; Beyer, R.; Rose, E.; Dressel, M.; Schlueter, J.A.; Turunova, S.A.; Zhilyaeva, E.I.; Lyubovskaya, R.N. Metallic state and charge-order metal-insulator transition in the quasi-two-dimensional conductor κ-$(BEDT\text{-}TTF)_2Hg(SCN)_2Cl$. *Phys. Rev. B* **2014**, *89*, 075133. [CrossRef]
38. Drichko, N.; Hackl, R.; Schlueter, J.A. Antiferromagnetic fluctuations in a quasi-two-dimensional organic superconductor detected by Raman spectroscopy. *Phys. Rev. B* **2015**, *92*, 161112.
39. Valentine, M.E.; Koohpayeh, S.; Phelan, W.A.; McQueen, T.M.; Rosa, P.F.S.; Fisk, Z.; Drichko, N. Breakdown of the Kondo insulating state in SmB_6 by introducing Sm vacancies. *Phys. Rev. B* **2016**, *94*, 075102. [CrossRef]
40. Kawamoto, A.; Miyagawa, K.; Nakazawa, Y.; Kanoda, K. ^{13}C NMR Study of Layered Organic Superconductors Based on BEDT-TTF Molecules. *Phys. Rev. Lett.* **1995**, *74*, 3455–3458.
41. Nakamura, Y.; Yoneyama, N.; Sasaki, T.; Tohyama, T.; Nakamura, A.; Kishida, H. Magnetic Raman Scattering Study of Spin Frustrated Systems, κ-(BEDT-TTF)2X. *J. Phys. Soc. Jpn.* **2014**, *83*, 074708.
42. Gati, E.; Fischer, J.K.; Lunkenheimer, P.; Zielke, D.; Köhler, S.; Kolb, F.; von Nidda, H.A.K.; Winter, S.M.; Schubert, H.; Schlueter, J.A.; et al. Evidence for electronically-driven ferroelectricity in the family of strongly correlated dimerized BEDT-TTF molecular conductors. *arXiv* **2017**, arXiv:1711.07384.
43. Ivek, T.; Beyer, R.; Badalov, S.; Čulo, M.; Tomić, S.; Schlueter, J.A.; Zhilyaeva, E.I.; Lyubovskaya, R.N.; Dressel, M. Metal-insulator transition in the dimerized organic conductor κ-$(BEDT\text{-}TTF)_2Hg(SCN)_2Br$. *Phys. Rev. B* **2017**, *96*, 085116. [CrossRef]
44. Powell, B.; Kenny, E.; Merino, J. Dynamical Reduction of the Dimensionality of Exchange Interactions and the "Spin-Liquid" Phase of κ-$(BEDT\text{-}TTF)_2X$. *Phys. Rev. Lett.* **2017**, *119*, 087204. [CrossRef] [PubMed]
45. Nakamura, Y.; Hiramatsu, T.; Yoshida, Y.; Saito, G.; Kishida, H. Optical Properties of a Quantum Spin Liquid Candidate Material, κ-$(BEDT\text{-}TTF)_2Ag_2(CN)_3$. *J. Phys. Soc. Jpn.* **2017**, *86*, 014710. [CrossRef]
46. Nakamura, Y.; Kato, R.; Kishida, H. Study of Magnetic Excitation in $Pd(dmit)_2$ Salts by Raman Scattering Spectroscopy. *J. Phys. Soc. Jpn.* **2015**, *84*, 044715. [CrossRef]